

Early neutron star evolution in high-mass X-ray binaries

Wynn C. G. Ho^{1,2*}, M. J. P. Wijngaarden,² Nils Andersson,² Thomas M. Tauris^{3,4} and F. Haberl⁵

¹*Department of Physics and Astronomy, Haverford College, 370 Lancaster Avenue, Haverford, PA, 19041, USA*

²*Mathematical Sciences and STAG Research Centre, University of Southampton, SO17 1BJ, Southampton, UK*

³*Aarhus Institute of Advanced Studies (AIAS), Aarhus University, Høegh-Guldbergs Gade 6B, 8000 Aarhus C, Denmark*

⁴*Department of Physics and Astronomy, Aarhus University, Ny Munkegade 120, 8000 Aarhus C, Denmark*

⁵*Max-Planck-Institut für extraterrestrische Physik, Giessenbachstraße, 85748 Garching, Germany*

Accepted 2020 March 5. Received 2020 March 3; in original form 2020 January 12

ABSTRACT

The application of standard accretion theory to observations of X-ray binaries provides valuable insights into neutron star properties, such as their spin period and magnetic field. However, most studies concentrate on relatively old systems, where the neutron star is in its late propeller, accretor, or nearly spin equilibrium phase. Here we use an analytic model from standard accretion theory to illustrate the evolution of high-mass X-ray binaries early in their life. We show that a young neutron star is unlikely to be an accretor because of the long duration of ejector and propeller phases. We apply the model to the recently discovered ~ 4000 yr old high-mass X-ray binary XMMU J051342.6–672412 and find that the system’s neutron star, with a tentative spin period of 4.4 s, cannot be in the accretor phase and has a magnetic field $B >$ a few $\times 10^{13}$ G, which is comparable to the magnetic field of many older high-mass X-ray binaries and is much higher than the spin equilibrium inferred value of a few $\times 10^{11}$ G. The observed X-ray luminosity could be the result of thermal emission from a young cooling magnetic neutron star or a small amount of accretion that can occur in the propeller phase.

Key words: accretion, accretion discs – pulsars: general – stars: magnetic field – stars: neutron – X-rays: binaries – X-rays: individual objects: XMMU J051342.6–672412.

1 INTRODUCTION

High-mass X-ray binaries (HMXBs) have typical ages of $\sim 10^6 - 10^7$ yr, based on the main sequence and post-main sequence lifetimes of the high-mass companion star. However, for a few HMXBs, an association with a supernova remnant has been made, which limits their age to $< 10^5$ yr (Haberl et al. 2012; Hénault-Brunet et al. 2012; Seward et al. 2012; Heinz et al. 2013; Gvaramadze et al. 2019; Maitra et al. 2019). Possibly the youngest HMXB is the one recently discovered near the geometrical centre of the supernova remnant MCSNR J0513–6724, with an age of $\approx 3800_{-900}^{+1900}$ yr. This HMXB, which we name XMMU J051342.6–672412 based on the coordinates derived using *XMM-Newton* data, has X-ray luminosity $\sim 7 \times 10^{33}$ erg s^{−1} and a likely neutron star (NS) component with a spin period of 4.4 s (Maitra et al. 2019). Detections of young HMXBs provide snapshots early in the accretion history and spin evolution of NS/pulsars and can yield valuable insights into

a hitherto unknown stage of HMXB evolution and accretion theory.

Most NSs are inferred to be born with a magnetic field $B \sim 10^{13}$ G and spin period $P \sim 100$ ms (e.g., Faucher-Giguère & Kaspi 2006; Gullón et al. 2014). For example, the ~ 1000 yr old Crab Pulsar has $B = 4 \times 10^{12}$ G and $P = 33$ ms. Traditional NS accretion theory dictates that this spin period is too short to allow matter inflowing at a rate \dot{M} to accrete onto the NS because it cannot penetrate the pulsar light cylinder, which is at distance

$$r_c = c/\Omega = 48 \text{ km} (P/1 \text{ ms}), \quad (1)$$

where $\Omega \equiv 2\pi/P$ (Shvartsman 1971; Illarionov & Sunyaev 1975; Lipunov 1992). In other words, for spin periods

$$P < 2\pi r_m/c = 150 \text{ ms} B_{13}^{4/7} \dot{M}_{-10}^{-2/7}, \quad (2)$$

r_c is smaller than the size of the magnetosphere, and the NS is in the *ejector* phase. Here we adopt the conventional approximation for magnetosphere size (e.g., Pringle & Rees

* E-mail: wynnho@slac.stanford.edu

1972; Lamb et al. 1973; Davidson & Ostriker 1973)

$$r_m = \xi r_A = \xi \left(\frac{\mu^4}{8GM\dot{M}^2} \right)^{1/7} = 7.0 \times 10^3 \text{ km } B_{13}^{4/7} \dot{M}_{-10}^{-2/7}, \quad (3)$$

where $\xi \approx 0.5$ (e.g., Ghosh & Lamb 1979; Wang 1996; Campana et al. 2018; Chashkina et al. 2019; Vasilopoulos et al. 2020), the Alfvén radius r_A is derived from balancing the ram pressure of accreting matter with pressure of the pulsar magnetic field, $\mu = BR^3/2$ is the magnetic dipole moment¹, $B_{13} = B/10^{13} \text{ G}$, $\dot{M}_{-10} = \dot{M}/10^{-10} M_\odot \text{ yr}^{-1}$, and we assume a NS mass $M = 1.4 M_\odot$ and radius $R = 10 \text{ km}$. Once the NS slows down sufficiently by electromagnetic dipole radiation, matter enters the light cylinder but is still unable to accrete onto the NS surface due to the centrifugal barrier. Instead, the pulsar is spun down by the torque of matter being flung out when r_m is greater than the corotation radius

$$r_{co} = \left(GM/\Omega^2 \right)^{1/3} = 17 \text{ km } (P/1 \text{ ms})^{2/3}, \quad (4)$$

and the pulsar is in the *propeller* phase. Once $r_m \lesssim r_{co}$, the pulsar can be spun-up by gaining the angular momentum carried by infalling matter in the *accretor* phase. We note that, when $r_m \sim r_{co}$ (with the precise values being uncertain, depending on the critical fastness parameter $\hat{\omega}_s$; Elsner & Lamb 1977; Ghosh & Lamb 1979; Wang 1995), spin-down and spin-up torques balance such that the net torque on the pulsar is nearly zero, the spin period does not change, and the pulsar is in *spin equilibrium* (Davidson & Ostriker 1973; Illarionov & Sunyaev 1975). The fastness parameter $\hat{\omega}_s \equiv \Omega/\Omega_K(r_m)$, where the Keplerian orbital frequency $\Omega_K(r_m)$ at the magnetosphere radius has the corresponding (spin equilibrium) period

$$P_{eq} = \frac{2\pi}{\Omega_K(r_m)} = \left(\frac{4\pi^2 r_m^3}{GM} \right)^{1/2} = 8.5 \text{ s } B_{13}^{6/7} \dot{M}_{-10}^{-3/7}. \quad (5)$$

In real systems, small variations in accretion rate can cause small spin period time derivatives \dot{P} and deviations from spin equilibrium. This may result in accretion onto the NS surface, as seen in observations, as well as in numerical simulations which model three-dimensional structure, viscosity, mass loss, and other effects (e.g., Lovelace et al. 1995; Romanova et al. 2004; Shakura et al. 2012; Tauris et al. 2012; Shi et al. 2015; Parfrey et al. 2017). The characteristic lengthscales (r_{lc} , r_m , and r_{co}) are plotted for $B = 10^{13} \text{ G}$ and $\dot{M} = 10^{-10} M_\odot \text{ yr}^{-1}$ in Figure 1, where we also highlight the ejector, propeller, and accretor/spin-equilibrium phases implied by the relative values of r_{lc} , r_m , and r_{co} . For systems evolving with mass-transfer via Roche-lobe overflow, spin equilibrium is disrupted again at the Roche-lobe decoupling phase (Tauris 2012).

In this work, we use the simple analytic spin period evolution model of Ho & Andersson (2017), which is based on standard accretion theory (see, e.g., Ghosh & Lamb 1979; Wang 1987; Lipunov 1992), to illustrate the evolution of the

¹ Note the factors of 8 and 2 in the denominator of r_m and μ , respectively, in contrast to other definitions in the literature which have different factors of order unity; this implies that derived values of various parameters such as B can differ by a factor of a few if these alternative definitions are used.

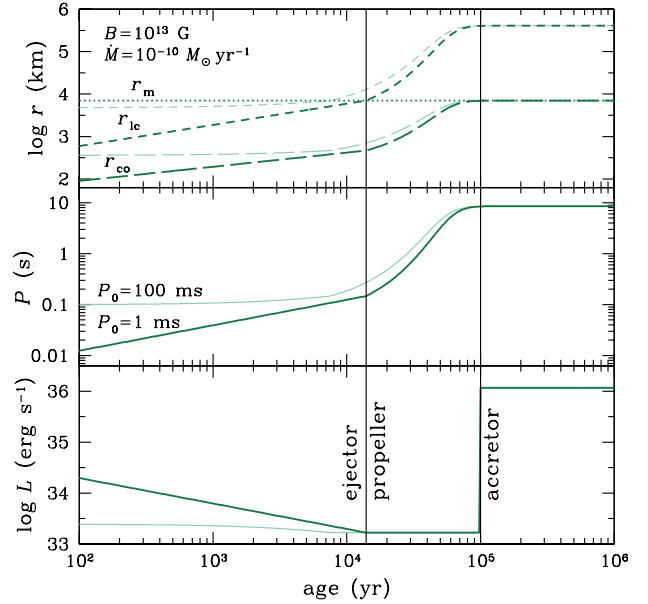


Figure 1. Top panel: Evolution of light cylinder radius r_{lc} (short-dashed), magnetosphere radius r_m (dotted), and corotation radius r_{co} (long-dashed) for constant magnetic field $B = 10^{13} \text{ G}$, constant accretion rate $\dot{M} = 10^{-10} M_\odot \text{ yr}^{-1}$, and initial spin periods $P = 1$ (dark) and 100 ms (light). Vertical lines separate ejector ($r_m > r_{lc}$), propeller ($r_{co} < r_m < r_{lc}$), and accretor/spin-equilibrium phases ($r_m \lesssim r_{co}$). Middle panel: Spin period evolution as determined by equations (7) and (12). Bottom panel: Luminosity evolution as determined by equation (13).

NS in HMXBs and expected accretion state of these systems, especially young ones like XMMU J051342.6–672412. Section 2 describes the evolution model. Section 3 applies the model to XMMU J051342.6–672412. Section 4 summarizes our work and discusses implications and some of the model assumptions.

2 MODEL FOR SPIN EVOLUTION AND ACCRETION PHASES

As mentioned in Section 1, a pulsar in the ejector phase does not interact with accreting matter and spins down as if in isolation, i.e., by emission of dipole radiation, such that $d\Omega/dt = -\beta\Omega^3$, where

$$\beta \equiv 2\mu^2/3c^3I = B^2R^6/6c^3I = 6.2 \times 10^{-16} \text{ s } B_{13}^2 \quad (6)$$

and we assume a NS moment of inertia $I = 10^{45} \text{ g cm}^2$. For simplicity, we use the traditional vacuum dipole formula of Pacini (1968); Gunn & Ostriker (1969) and consider an orthogonal rotator. Thus the spin evolution from an initial spin rate $\Omega_0 (= 2\pi/P_0)$ is

$$\Omega = \Omega_0 \left(1 + 2\beta\Omega_0^2 t \right)^{-1/2} = \Omega_0 (1 + t/t_{em})^{-1/2} \quad \text{for } t < t_{ej}, \quad (7)$$

where

$$t_{em} = 1/(2\beta\Omega_0^2) = 0.65 \text{ yr } B_{13}^{-2} (P_0/1 \text{ ms}). \quad (8)$$

The ejector phase lasts until $t = t_{\text{ej}}$ when $r_m = r_{\text{lc}}$, where equations (2) and (7) give

$$t_{\text{ej}} = t_{\text{em}} \left[\left(\frac{\Omega_0 r_m}{c} \right)^2 - 1 \right] \approx \frac{r_m^2}{2\beta c^2} = 1.4 \times 10^4 \text{ yr } B_{13}^{-6/7} \dot{M}_{-10}^{-4/7}. \quad (9)$$

Once the propeller phase begins, the spin evolution is governed approximately by (e.g., Illarionov & Sunyaev 1975; Alpar 2001; Ho et al. 2014; Ho & Andersson 2017; see also Parfrey et al. 2016)

$$I \frac{d\Omega}{dt} = -\dot{M} r_m^2 [\Omega - \Omega_K(r_m)] = \frac{I \Omega_K}{t_{\text{prop}}} (1 - \hat{\omega}_s), \quad (10)$$

where

$$t_{\text{prop}} \equiv I / \dot{M} r_m^2 = 1.0 \times 10^4 \text{ yr } B_{13}^{-8/7} \dot{M}_{-10}^{-3/7}. \quad (11)$$

One term is the propeller/spin-down torque, while the other term is the accretion/spin-up torque. A simple solution of equation (10) can be obtained by assuming constant μ and \dot{M} (and thus constant r_m and Ω_K), yielding

$$\Omega = [\Omega_{\text{ej}} - \Omega_K(r_m)] e^{-(t-t_{\text{ej}})/t_{\text{prop}}} + \Omega_K(r_m) \quad \text{for } t > t_{\text{ej}}, \quad (12)$$

where $\Omega_{\text{ej}} \equiv c/r_m$ is the spin frequency corresponding to the critical spin period marking the end of the ejector phase and beginning of the propeller phase [see equation (2)]. One can see from equation (12) that, once the spin rate evolves to the point when $r_{\text{co}} = r_m$, the term in brackets cancel and the spin period is constant at the spin equilibrium value P_{eq} given by equation (5).

Equations (7) and (12) describe the complete evolution of NS spin frequency (or spin period) from the ejector phase, through to the propeller phase, and then to the accretor/spin equilibrium phase. The middle panel of Figure 1 shows this evolution for a NS with $B = 10^{13}$ G, $\dot{M} = 10^{-10} M_{\odot} \text{ yr}^{-1}$ and initial spin periods $P_0 = 1$ and 100 ms. As is clear, the choice of initial spin period makes no difference to the evolution of the spin period at later times, such as in the accretor phase.

We can obtain an estimate of the HMXB luminosity during the different accretion phases due simply to gravitational infall

$$L = G M \dot{M} / r = 1.2 \times 10^{36} \text{ erg s}^{-1} \dot{M}_{-10} (10 \text{ km}/r), \quad (13)$$

where $r = r_{\text{lc}}$ during the ejector phase, $r = r_m$ during the propeller phase, and $r = R$ during the accretor/spin equilibrium phase, and no beaming is assumed (e.g., King & Cominsky 1994; Stella et al. 1994). Two examples are shown in the bottom panel of Figure 1. The above estimate assumes the accretion flow is cold and does not radiate on its own and thus represents a minimum luminosity, as other emission processes could contribute and dominate the observed flux from an accreting system.

The dependence of spin period evolution on magnetic field B and accretion rate \dot{M} is illustrated in Figure 2. Also plotted are radio pulsar death lines, above which radio emission is thought to be inoperative (Sturrock 1971; Ruderman & Sutherland 1975). The exact location and dependencies of the death line are uncertain, and we simply use $P = 7.7 \text{ s } B_{13}^{1/2}$ from Bhattacharya et al. (1992); for alternative death lines, see, e.g., Chen & Ruderman (1993); Zhang et al. (2000); Hibschan & Arons (2001). One can see that, in some cases, even if radio emission is not suppressed by accretion, radio emission would still be inactive.

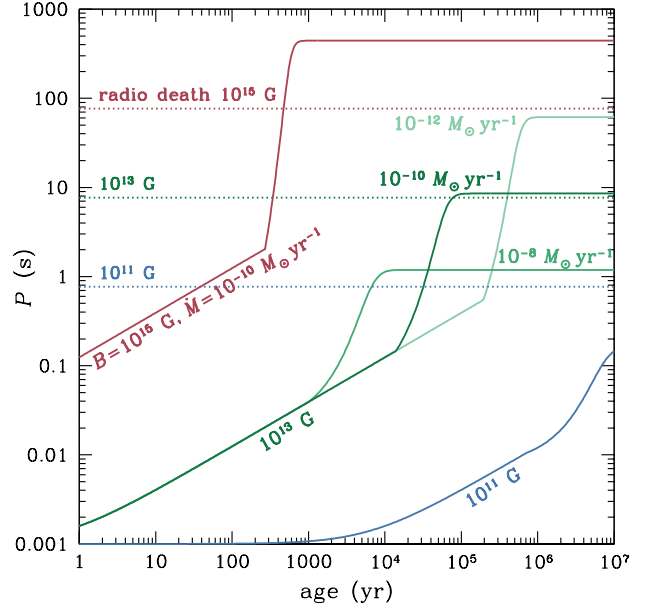


Figure 2. Spin period as a function of time, starting from ejector phase onset at $P_0 = 1$ ms, for magnetic fields $B = 10^{11}$, 10^{13} , and 10^{15} G and accretion rate $\dot{M} = 10^{-10} M_{\odot} \text{ yr}^{-1}$ and for $B = 10^{13}$ G and $\dot{M} = 10^{-12}$ and $10^{-8} M_{\odot} \text{ yr}^{-1}$. Horizontal dotted lines indicate the theoretically uncertain death line for radio pulsar emission for the magnetic fields shown.

3 APPLICATION TO XMMU J051342.6–672412

In this section, we apply the simple accretion model to the youngest NS with a known spin period in a HMXB, XMMU J051342.6–672412. Maitra et al. (2019) recently identified XMMU J051342.6–672412 as a HMXB at the center of the Large Magellanic Cloud supernova remnant MC-SNR J0513–6724. The size of the supernova remnant yields an age of 3800^{+1900}_{-900} yr. An OGLE light curve shows the B2.5Ib optical counterpart to have a 2.2 d periodicity, which is interpreted as the orbital period. XMM-Newton data reveal pulsations at 4.4 s, which is interpreted as the NS spin period, and a power law spectrum with a 0.2–12 keV luminosity of $7 \times 10^{33} \text{ erg s}^{-1}$ (at 50 kpc). Maitra et al. (2019) then attribute the measured luminosity to matter accreting onto the NS surface [equation (13) with $r = R$], which implies a mass accretion rate of $\dot{M} = 6 \times 10^{-13} M_{\odot} \text{ yr}^{-1}$, and derive a magnetic field $B \sim 4 \times 10^{11}$ G, assuming the NS is at spin equilibrium [using equation (5)].

This result for XMMU J051342.6–672412 is problematic in standard accretion theory because the described scenario does not account for evolution. If the magnetic field is indeed as low as $\sim 4 \times 10^{11}$ G, then the duration of the ejector phase from equation (9) is $t_{\text{ej}} = 2 \times 10^5 \text{ yr } \dot{M}_{-10}^{-4/7}$, and this would only be comparable to the age of XMMU J051342.6–672412 for an accretion rate $\dot{M} \sim 10^{-7} M_{\odot} \text{ yr}^{-1}$, greatly exceeding the accretion rate onto the NS surface implied by the observed luminosity. On the other hand, with such a low field, the pulsar spin period would not have changed significantly from its value at birth, which means that it would have been born in the propeller phase [see equation (2)]. In fact, the propeller phase would also be long, with a timescale from

equation (11) of $t_{\text{prop}} = 4 \times 10^5 \text{ yr } \dot{M}_{-10}^{-3/7}$, unless the accretion rate is an even higher $\dot{M} \sim 5 \times 10^{-6} M_{\odot} \text{ yr}^{-1}$. In summary, with a magnetic field as low as a few $\times 10^{11}$ G, the NS in XMMU J051342.6–672412 would not have had enough time to slow down sufficiently to be in the accretor phase, unless the accretion rate greatly exceeds observations and expectations.

Let us apply the analytic model of Section 2, which qualitatively encapsulates standard accretion theory and evolution of accreting systems, to infer the possible accretion phase, magnetic field, and accretion rate of XMMU J051342.6–672412. In doing so, we must match the observed values of spin period $P = 4.4$ s and luminosity $7 \times 10^{33} \text{ erg s}^{-1}$ at an age of ≈ 2900 – 5700 yr. For simplicity, we do not apply a bolometric correction to the observed X-ray luminosity.

First, we consider what criteria are needed for XMMU J051342.6–672412 to be in the ejector phase. In this phase, energy loss from electromagnetic dipole radiation drives spin period evolution, which is described by equation (7). From age $= (P/2\pi)^2 / (2\beta)$, where $P = 4.4$ s and the age is 2900–5700 yr, we find that the magnetic field must be $B = (5 - 7) \times 10^{14}$ G. At greater fields strengths, spin-down is too effective, and XMMU J051342.6–672412 would have a much longer spin period at the current age. The accretion rate must also be low enough such that the current spin period is below the limit needed to initiate the propeller phase. From equation (2), we find that $\dot{M} < 2 \times 10^{-12} M_{\odot} \text{ yr}^{-1}$. Finally, the light cylinder radius $r_{\text{c}} = 2.1 \times 10^5 \text{ km}$, such that the accretion luminosity is $L = 6 \times 10^{31} \text{ erg s}^{-1}$, which is well below the observed luminosity.

From the above discussion, we expect that if the magnetic field is below that of the ejector phase and accretion rate is higher, then the NS will be in the propeller state. The shaded region in Figure 3 illustrates the relation between B and \dot{M} needed to solve the evolution given by equation (12), i.e.,

$$\ln \frac{\Omega_{\text{ej}} - \Omega_{\text{K}}}{\Omega - \Omega_{\text{K}}} = \frac{|\text{age} - t_{\text{ej}}|}{t_{\text{prop}}}, \quad (14)$$

for XMMU J051342.6–672412. Regions where values of B – \dot{M} would produce an accretor and ejector are also indicated in Figure 3.

Figure 4 shows evolutions of spin period (upper panel) and luminosity (lower panel) for various combinations of magnetic field B and accretion rate \dot{M} that lead to ejector and propeller phases for XMMU J051342.6–672412 (see Figure 3). Note that the relatively low $B = 10^{13}$ G evolution is for the accretor phase but only at an age much older than that of XMMU J051342.6–672412. The evolution of this case produces a luminosity which exceeds that seen from XMMU J051342.6–672412.

The origin of XMMU J051342.6–672412’s observed pulsed X-ray luminosity ($L_{\text{X}} \sim 7 \times 10^{33} \text{ erg s}^{-1}$) is uncertain. If the NS is in the propeller phase, then the accretion luminosity [equation (13)] at the magnetosphere would match the observed X-ray luminosity for $B \approx (3 - 6) \times 10^{13}$ G, although the temperature at the relevant $r_{\text{m}} (\sim 10^4 \text{ km})$ is probably too low to result in much X-ray emission. But even in the propeller phase, a small amount of matter can reach the NS surface intermittently (Romanova et al. 2004, 2018; D’Angelo & Spruit 2010, 2012) since the centrifugal barrier only applies to the closed portion of the magnetosphere, and

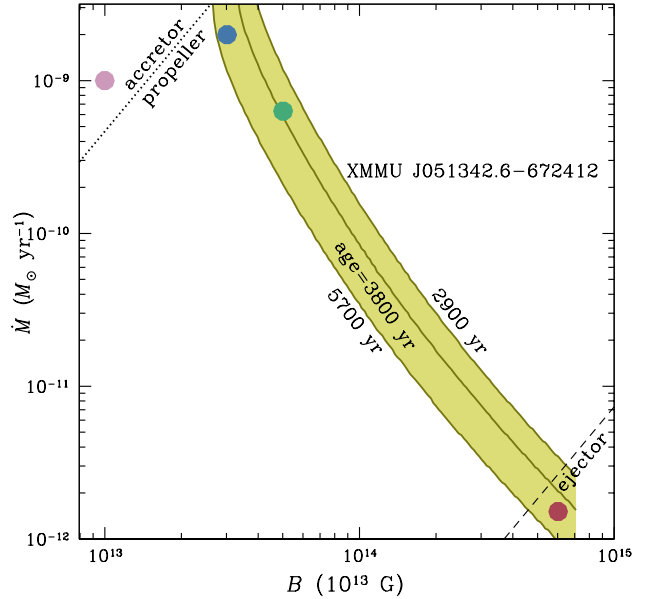


Figure 3. Constraints on the magnetic field B and accretion rate \dot{M} of XMMU J051342.6–672412. The shaded region denotes B and \dot{M} values which produce a NS with the observed 4.4 s spin period at the 2900–5800 yr age of XMMU J051342.6–672412. Colored filled circles denote combinations of B and \dot{M} whose spin period and luminosity evolutions are shown in Figure 4. Dotted line and short-dashed line separate regions where the NS is in accretor, propeller, and ejector phases.

the X-ray luminosity of XMMU J051342.6–672412 would imply a low residual accretion rate $\sim 6 \times 10^{-13} M_{\odot} \text{ yr}^{-1}$, which is comparable to (uncertain) theoretical estimates in the strong ($\dot{\omega}_{\text{s}} \gg 1$) propeller regime (e.g., Lipunov & Shakura 1976; Menou et al. 1999; see also Güngör et al. 2017). On the other hand, if the NS is in the accretor phase, then accretion directly onto the NS surface at $\dot{M} > 3 \times 10^{-9} M_{\odot} \text{ yr}^{-1}$ (see Figure 3) would produce $L_{\text{X}} > 4 \times 10^{37} \text{ erg s}^{-1}$. Another possibility is that XMMU J051342.6–672412 emits like young rotation-powered pulsars, which can produce pulsed non-thermal X-rays from their magnetosphere and pulsar wind nebula with X-ray luminosities $< 10^{-2} \dot{E}$, where $\dot{E} = I \Omega \dot{\Omega}$ is spin-down power (Becker & Trümper 1997; Enoto et al. 2019). The two intermediate cases shown in Figure 4 have too low \dot{E} ($\sim 10^{35} \text{ erg s}^{-1}$), but it is important to remember that the L_{X} – \dot{E} correlation holds for rotation-powered pulsars. Finally, we find that a 0.41 keV blackbody model can fit the spectra of XMMU J051342.6–672412 slightly better than the power law model fit of Maitra et al. (2019) (blackbody C-statistic = 117.3 versus power law C-statistic = 124.6 for 126 degrees of freedom). The resulting 1 km emission radius could indicate thermal radiation from a hot spot on the NS surface, and a strong surface magnetic field can contribute to generating the observed strong pulsations (see, e.g., PSR J1119–6127; Ng et al. 2012). Thus the bulk of X-rays from XMMU J051342.6–672412 could be thermal emission from a young X-ray dim isolated NS (XDINS) or magnetar since both share some similar properties, e.g., XDINSs and magnetars have $P \approx 2 - 17$ s, $B > 10^{13}$ G, and quiescent X-ray luminosity $\sim 10^{31} - 10^{36} \text{ erg s}^{-1}$ (Haberl 2007;

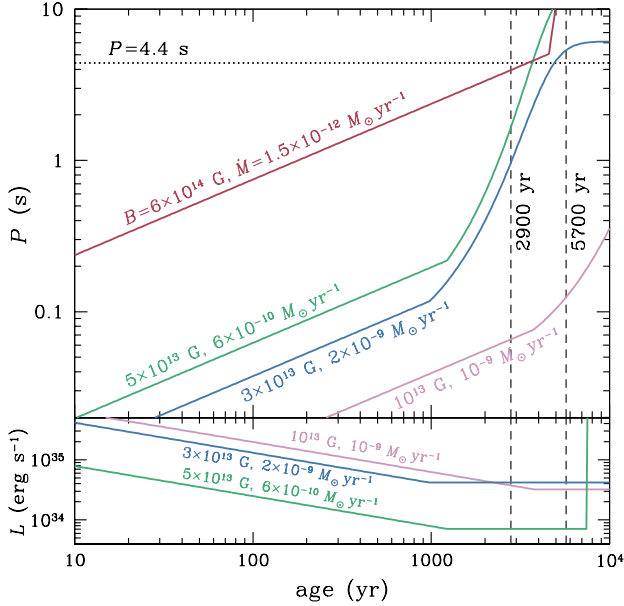


Figure 4. Top panel: Spin period evolutions for magnetic field and accretion rate [$B(\text{G}), \dot{M}(M_{\odot} \text{ yr}^{-1})$] = [$10^{13}, 10^{-9}$], [$3 \times 10^{13}, 2 \times 10^{-9}$], [$5 \times 10^{13}, 6 \times 10^{-10}$], and [$6 \times 10^{14}, 1.5 \times 10^{-12}$] and $P_0 = 1$ ms. Horizontal dotted line indicates the current 4.4 s spin period of XMMU J051342.6–672412, and vertical dashed lines denote bounds on its age. Bottom panel: Luminosity evolutions corresponding to the spin period evolutions shown in the top panel, where luminosity is calculated using equation (13) and $r = r_{\text{c}}$ during the ejector phase, $r = r_{\text{m}}$ during the propeller phase, and $r = R$ during the accretor/spin equilibrium phase. The luminosity evolution for [$6 \times 10^{14}, 1.5 \times 10^{-12}$] is below the luminosity range displayed.

Turolla 2009; Kaspi & Beloborodov 2017; Enoto et al. 2019; Hu et al. 2019).

4 DISCUSSION

In this work, we considered a simple analytic model that follows from standard accretion theory (see also Ho & Andersson 2017). We showed how the NS spin period evolves during ejector and propeller phases, until reaching accretor and spin equilibrium phases, and provide estimates of the ejector phase duration and propeller phase timescale. We also estimated the evolution of accretion luminosity, which scales as $1/r$, where r can be equal to the light cylinder radius r_{c} , magnetosphere radius r_{m} , or NS radius R during ejector, propeller, or accretor/spin equilibrium phases, respectively. Applying this model to the recently discovered young HMXB XMMU J051342.6–672412, we inferred that the NS is likely to be in the propeller phase and that the NS has a magnetic field $B > \text{a few} \times 10^{13}$ G. This magnetic field is stronger than, but comparable to, the magnetic field measured or inferred in many other HMXBs (e.g., Ho et al. 2014; Staubert et al. 2019). The observed X-ray luminosity could be due to thermal emission from the magnetised surface of this young cooling NS or a small amount of matter that leaks through the centrifugal barrier and accretes onto the NS surface.

While the simple model is based on fundamentals of standard accretion theory, caution must be exercised in using the precise results. Real accreting systems are complex and require detailed modeling and numerical simulations for accurate quantitative solutions (see, e.g., Lovelace et al. 1995; Romanova et al. 2004, 2018; Parfrey et al. 2017). For example, Shakura et al. (2015) develop a more detailed model of wind accretion onto a NS in HMXB systems. They distinguish between two main regimes: Supersonic (Bondi-Hoyle-Lyttleton) accretion when captured matter cools rapidly and falls supersonically towards the NS magnetosphere and subsonic (settling) accretion when captured hot plasma reaches the magnetosphere boundary. In the first regime, shocked matter cools via Compton processes and enters the magnetosphere due to Rayleigh-Taylor instabilities (Arons & Lea 1976). The accreting NS can either spin up or spin down, depending on whether the wind carries prograde or retrograde angular momentum when entering the magnetosphere (see also Shapiro & Lightman 1976; Wang 1981; Klus et al. 2014). In the second regime, matter remains hot since the plasma cooling time is much longer than the free-fall time, and a quasi-static shell forms around the magnetosphere leading to subsonic accretion. In this case, both spin-up and spin-down can occur even if the specific angular momentum of the wind is only prograde. Shakura et al. (2015) argue that triggering of the transition from supersonic to subsonic accretion may be related to a switch in the X-ray beam pattern in response to a change in optical depth, i.e., the X-ray beam pattern changes with decreasing X-ray luminosity (near 4×10^{36} erg s $^{-1}$) from a fan beam to a pencil beam. Observational evidence to support this hypothesis is found in pulse profile observations of Vela X-1 in different energy bands (Doroshenko et al. 2011).

In the case of XMMU J051342.6–672412, $L_X \sim 7 \times 10^{33}$ erg s $^{-1}$ and the plasma is expected to remain hot until it reaches the magnetosphere boundary. As a consequence, the effective gravitational acceleration changes above the magnetosphere, and the average radial velocity of the settling plasma is expected to be smaller than the standard free-fall velocity ($= \sqrt{2GM/r}$). This correction would produce some changes in our numerical results. Moreover, the effects of a complicated non-stationary accretion wake (El Mellah & Casse 2015; de Val-Borro et al. 2017) and a trapped disc with cyclic accretion (D’Angelo & Spruit 2012) are difficult to quantify, and a full treatment of these effects is beyond the scope of this paper.

Other caveats are our assumptions of constant accretion rate and magnetic field throughout the various accretion phases. Modelling of stellar evolution in binaries shows that the wind mass-loss rate, and thus mass-transfer rate, varies significantly over time (Langer 2012). This is also true for mass transfer via Roche-lobe overflow (Tauris et al. 2012). Meanwhile, the magnetic field of an accreting NS is expected to decay, e.g., as a consequence of heating of the crust, which reduces its electrical conductivity (Romani 1990; Bhattacharya 2002). On the other hand, a magnetic field that is increasing at the present time could be the result of an early episode of field burial by accretion at very high rates (in order to prevent field re-emergence on short timescales; Chevalier 1989; Geppert et al. 1999; Bernal et al. 2010; Ho 2011, 2015; Viganò & Pons 2012). However, a re-emerging magnetic field would not allow XMMU J051342.6–672412

to be in the accretor phase at the current time since the field would have been weaker in the past. A weak field would produce a long timescale for spin-down [equation (8)]. Thus XMMU J051342.6–672412 would not reach the current spin period of 4.4 s if it was born at typical birth periods of less than one second (if XMMU J051342.6–672412 was born near its current period, the propeller timescale at these weak fields is longer than the current age; see discussion in Section 3). A time-varying accretion rate (see, e.g., Tauris et al. 2012; Bhattacharyya & Chakrabarty 2017; D’Angelo 2017; Mushtukov et al. 2019) might yield a solution such that XMMU J051342.6–672412 is in the accretor phase and have a weak field, but this would require fine-tuning. For example, a very high accretion rate at early times could cause cessation of the ejector phase, but this would also shorten the propeller phase such that the accretor/spin equilibrium phase would begin at much shorter periods than the current spin period.

Circinus X-1 is another (possible) HMXB in a young (< 4600 yr) supernova remnant (Heinz et al. 2013). Circinus X-1 is identified as a NS system because it is seen to undergo Type I X-ray bursts (Tennant et al. 1986; Linares et al. 2010), which occur in many accreting low magnetic field NSs in a low-mass X-ray binary. In contrast to XMMU J051342.6–672412, the spin period of Circinus X-1 is not known, and its highly variable X-ray luminosity can exceed 10^{38} erg s⁻¹ (Linares et al. 2010; Heinz et al. 2015). A scenario in which Circinus X-1 has $B \sim 10^{13}$ G and $\dot{M} \sim 10^{-8} M_{\odot}$ yr⁻¹ and was born somewhat below its spin equilibrium period of 1 s would imply the NS started in the propeller phase, with a timescale of ~ 1000 yr, and is now entering its accretor/spin equilibrium phase. For lower long-term accretion rates, a somewhat stronger magnetic field would still yield the same result.

Finally one could consider applying the model described here to low-mass X-ray binary (LMXB) systems. LMXBs have much lower magnetic fields ($B \sim 10^8 - 10^9$ G), which yield long ejector and propeller timescales, $t_{ej} \sim 10^8$ yr and $t_{prop} \sim 10^9$ yr, respectively. However, since LMXBs are likely to be very old, it may be unlikely for us to observe them early enough in their accretion history to see potential effects of ejector and early propeller phases.

ACKNOWLEDGEMENTS

The authors thank the anonymous referee for comments which led to improvements in the manuscript. WCGH and NA acknowledge support through grant ST/R00045X/1 from the Science and Technology Facilities Council in the United Kingdom. TMT acknowledges an AIAS-COFUND Senior Fellowship funded by the European Union Horizon 2020 Research and Innovation Programme (grant agreement no. 754513) and Aarhus University Research Foundation.

REFERENCES

Alpar M. A., 2001, *ApJ*, **554**, 1245
 Arons J., Lea S. M., 1976, *ApJ*, **207**, 914
 Becker W., Trümper J., 1997, *A&A*, **326**, 682

Bernal C. G., Lee W. H., Page D., 2010, *Rev. Mex. Astron. Astrofis.*, **46**, 309
 Bhattacharya D., 2002, *Journal of Astrophysics and Astronomy*, **23**, 67
 Bhattacharya D., Wijers R. A. M. J., Hartman J. W., Verbunt F., 1992, *A&A*, **254**, 198
 Bhattacharyya S., Chakrabarty D., 2017, *ApJ*, **835**, 4
 Campana S., Stella L., Mereghetti S., de Martino D., 2018, *A&A*, **610**, A46
 Chashkina A., Lipunova G., Abolmasov P., Poutanen J., 2019, *A&A*, **626**, A18
 Chen K., Ruderman M., 1993, *ApJ*, **402**, 264
 Chevalier R. A., 1989, *ApJ*, **346**, 847
 D’Angelo C. R., 2017, *MNRAS*, **470**, 3316
 D’Angelo C. R., Spruit H. C., 2010, *MNRAS*, **406**, 1208
 D’Angelo C. R., Spruit H. C., 2012, *MNRAS*, **420**, 416
 Davidson K., Ostriker J. P., 1973, *ApJ*, **179**, 585
 Doroshenko V., Santangelo A., Suleimanov V., 2011, *A&A*, **529**, A52
 El Mellah I., Casse F., 2015, in SF2A-2015: Proceedings of the Annual meeting of the French Society of Astronomy and Astrophysics. pp 325–331
 Elsner R. F., Lamb F. K., 1977, *ApJ*, **215**, 897
 Enoto T., Kisaka S., Shibata S., 2019, *Reports on Progress in Physics*, **82**, 106901
 Faucher-Giguère C.-A., Kaspi V. M., 2006, *ApJ*, **643**, 332
 Geppert U., Page D., Zannias T., 1999, *A&A*, **345**, 847
 Ghosh P., Lamb F. K., 1979, *ApJ*, **234**, 296
 Gullón M., Miralles J. A., Viganò D., Pons J. A., 2014, *MNRAS*, **443**, 1891
 Güngör C., Ekşi K. Y., Göğüş E., Güver T., 2017, *ApJ*, **848**, 13
 Gunn J. E., Ostriker J. P., 1969, *Nature*, **221**, 454
 Gvaramadze V. V., Kniazev A. Y., Oskinova L. M., 2019, *MNRAS*, **485**, L6
 Haberl F., 2007, *Ap&SS*, **308**, 181
 Haberl F., Sturm R., Filipović M. D., Pietsch W., Crawford E. J., 2012, *A&A*, **537**, L1
 Heinz S., et al., 2013, *ApJ*, **779**, 171
 Heinz S., et al., 2015, *ApJ*, **806**, 265
 Hénault-Brunet V., et al., 2012, *MNRAS*, **420**, L13
 Hirschman J. A., Arons J., 2001, *ApJ*, **554**, 624
 Ho W. C. G., 2011, *MNRAS*, **414**, 2567
 Ho W. C. G., 2015, *MNRAS*, **452**, 845
 Ho W. C. G., Andersson N., 2017, *MNRAS*, **464**, L65
 Ho W. C. G., Klus H., Coe M. J., Andersson N., 2014, *MNRAS*, **437**, 3664
 Hu C.-P., Ng C. Y., Ho W. C. G., 2019, *MNRAS*, **485**, 4274
 Illarionov A. F., Sunyaev R. A., 1975, *A&A*, **39**, 185
 Kaspi V. M., Beloborodov A. M., 2017, *ARA&A*, **55**, 261
 King A., Cominsky L., 1994, *ApJ*, **435**, 411
 Klus H., Ho W. C. G., Coe M. J., Corbet R. H. D., Townsend L. J., 2014, *MNRAS*, **437**, 3863
 Lamb F. K., Pethick C. J., Pines D., 1973, *ApJ*, **184**, 271
 Langer N., 2012, *ARA&A*, **50**, 107
 Linares M., et al., 2010, *ApJ*, **719**, L84
 Lipunov V. M., 1992, *Astrophysics of Neutron Stars*. Springer-Verlag
 Lipunov V. M., Shakura N. I., 1976, *Soviet Astronomy Letters*, **2**, 133
 Lovelace R. V. E., Romanova M. M., Bisnovatyi-Kogan G. S., 1995, *MNRAS*, **275**, 244
 Maitra C., et al., 2019, *MNRAS*, **490**, 5494
 Menou K., Esin A. A., Narayan R., Garcia M. R., Lasota J.-P., McClintock J. E., 1999, *ApJ*, **520**, 276
 Mushtukov A. A., Lipunova G. V., Ingram A., Tsygankov S. S., Mönkkönen J., van der Klis M., 2019, *MNRAS*, **486**, 4061
 Ng C. Y., Kaspi V. M., Ho W. C. G., Weltevrede P., Bogdanov S., Shannon R., Gonzalez M. E., 2012, *ApJ*, **761**, 65

- Pacini F., 1968, *Nature*, **219**, 145
- Parfrey K., Spitkovsky A., Beloborodov A. M., 2016, *ApJ*, **822**, 33
- Parfrey K., Spitkovsky A., Beloborodov A. M., 2017, *MNRAS*, **469**, 3656
- Pringle J. E., Rees M. J., 1972, *A&A*, **21**, 1
- Romani R. W., 1990, *Nature*, **347**, 741
- Romanova M. M., Ustyugova G. V., Koldoba A. V., Lovelace R. V. E., 2004, *ApJ*, **616**, L151
- Romanova M. M., Blinova A. A., Ustyugova G. V., Koldoba A. V., Lovelace R. V. E., 2018, *New Astron.*, **62**, 94
- Ruderman M. A., Sutherland P. G., 1975, *ApJ*, **196**, 51
- Seward F. D., Charles P. A., Foster D. L., Dickel J. R., Romero P. S., Edwards Z. I., Perry M., Williams R. M., 2012, *ApJ*, **759**, 123
- Shakura N., Postnov K., Kochetkova A., Hjalmarsdotter L., 2012, *MNRAS*, **420**, 216
- Shakura N. I., Postnov K. A., Kochetkova A. Y., Hjalmarsdotter L., Sidoli L., Paizis A., 2015, *Astronomy Reports*, **59**, 645
- Shapiro S. L., Lightman A. P., 1976, *ApJ*, **204**, 555
- Shi C.-S., Zhang S.-N., Li X.-D., 2015, *ApJ*, **813**, 91
- Shvartsman V. F., 1971, *Soviet Ast.*, **15**, 342
- Staubert R., et al., 2019, *A&A*, **622**, A61
- Stella L., Campana S., Colpi M., Mereghetti S., Tavani M., 1994, *ApJ*, **423**, L47
- Sturrock P. A., 1971, *ApJ*, **164**, 529
- Tauris T. M., 2012, *Science*, **335**, 561
- Tauris T. M., Langer N., Kramer M., 2012, *MNRAS*, **425**, 1601
- Tennant A. F., Fabian A. C., Shafer R. A., 1986, *MNRAS*, **221**, 27
- Turolla R., 2009, in Becker W., ed., *Astrophysics and Space Science Library* Vol. 357, *Neutron Stars and Pulsars*. Springer-Verlag, pp 141–163, doi:10.1007/978-3-540-76965-1_7
- Vasilopoulos G., Lander S. K., Koliopoulos F., Bailyn C. D., 2020, *MNRAS*, **491**, 4949
- Viganò D., Pons J. A., 2012, *MNRAS*, **425**, 2487
- Wang Y. M., 1981, *A&A*, **102**, 36
- Wang Y. M., 1987, *A&A*, **183**, 257
- Wang Y. M., 1995, *ApJ*, **449**, L153
- Wang Y. M., 1996, *ApJ*, **465**, L111
- Zhang B., Harding A. K., Muslimov A. G., 2000, *ApJ*, **531**, L135
- de Val-Borro M., Karovska M., Sasselov D. D., Stone J. M., 2017, *MNRAS*, **468**, 3408

This paper has been typeset from a $\text{\TeX}/\text{\LaTeX}$ file prepared by the author.